Correspondence to:
A. Recking,
alain.recking@inrae.fr

Flow Resistance and Hydraulic Geometry in Gravel-And Boulder-Bed Rivers

Rob Ferguson[1] and **Alain Recking[2]**

[1]Department of Geography, Durham University, Durham, UK, [2]Univ. Grenoble Alpes, INRAE, CNRS, IRD, Grenoble INP, IGE, Grenoble, France

Abstract The frictional resistance of river beds affects how water discharge is partitioned between depth and velocity, which is important in many aspects of hydrology, geomorphology, and aquatic ecology. Many of the most widely-used resistance equations predict reach-average velocity from relative submergence (RS), the ratio of mean flow depth to a bed roughness height such as the 84th percentile of the bed grain-size distribution (D_{84}). Nondimensional hydraulic geometry (HG) is an alternative approach that directly partitions unit discharge into depth and velocity. We show that any RS equation has an implicit or explicit HG equivalent, and the other way round. Analysis of a large set of flow measurements in gravel- and boulder-bed channels confirms previous findings that HG equations using D_{84} outperform mathematically equivalent RS equations in predicting velocity. This paradox is explained by mathematical analysis and numerical experiments, both of which show that HG equations are less sensitive to the inevitable measurement uncertainty in the variables required for a prediction and the observed velocity used for testing. We also propose a new, simple and effective HG equation using D_{84} to predict depth and velocity from unit discharge. It is derived in the same way as the now widely-used variable-power equation equation (Ferguson, 2007, https://doi.org/10.1029/2006wr005422) and for deep flows it reduces to an inverted Manning-type equation. It should be possible to use HG equations for flow resistance in sand-bed and bedrock rivers, but this may require new definitions of roughness height.

Plain Language Summary The same volume of water flowing along a river can be slow and deep, or fast and shallow. This matters for flood risk locally and downstream, the river's ecosystem, and erosion of the bed. The outcome has long been known to depend on channel gradient (shallower flow on steeper slopes) and bed roughness (deeper flow on rougher beds), but there are many different equations for making quantitative predictions in specific circumstances. We show that equations predicting depth and speed from volume work better in tests than those predicting speed and volume from depth. This is because the first type is less affected by errors in the measurements required to make a prediction. We finish by recommending three specific equations for different purposes.

1. Introduction

Flow resistance equations are required for many aspects of river science and engineering, including flood risk assessment, aquatic habitat assessment, river restoration design, geomorphological modeling, and remote sensing of river discharge. There are two broad types of application, and correspondingly two types of equation.

The classic application is to predict a river's mean velocity, and thus also its discharge, from known or assumed values of mean depth. River velocity is determined by the balance between the gravity driving force and the frictional resistance of the channel, so two other variables are required: channel slope and some kind of roughness metric. The standard version of the Manning equation is of this type, and so are logarithmic equations inspired by boundary-layer theory (e.g., Bathurst, 1985; Hey, 1979; Keulegan, 1938) and the more recent variable-power equation (VPE) (Ferguson, 2007). Most such equations, including a dimensionally consistent version of the Manning equation, can be regarded as predicting the Darcy-Weisbach friction factor from the ratio of flow depth to a roughness height. We will refer to them as relative-submergence (RS) equations.

The other type of application involves predicting depth and velocity from a known or assumed discharge, as for example, in habitat assessment and river restoration or when estimating mean shear stress in geomorphological models that predict bedload transport or bedrock incision. An inverted form of the Manning equation is often used for this, since other RS equations cannot be inverted and must therefore be solved iteratively in this type of application. The other possibility is to use a so-called nondimensional hydraulic geometry (HG) resistance

equation. HG equations predict a nondimensional variable that includes velocity from another nondimensional variable that includes discharge (Comiti et al., 2007; Ferguson, 2007; Rickenmann & Recking, 2011). Tests by Ferguson (2007) and Rickenmann and Recking (2011) of the ability of alternative flow resistance equations to reproduce measured velocities in rivers with beds of gravel or coarser sediment had an unexpected result: HG resistance equations were more accurate than mathematically equivalent RS equations.

One of the aims of this paper is to explain this paradoxical finding. On the way to doing this, we make three other contributions: (a) We show that RS and HG resistance equations are mathematically equivalent, (b) we derive a new and simpler HG equation with which to partition discharge into depth and velocity, and (c) we confirm that HG equations perform better than RS equations at reproducing measured velocities in coarse-bed rivers. Our final contribution is (d) that the paradox is explained by the greater sensitivity of RS equations to measurement error or other uncertainty in the predictor variables or the observed velocity.

2. Background

Before considering the mathematical links between RS-type and HG-type resistance equations we include a summary of the RS approach and a brief history of the HG approach. We also explain how the definitions of the nondimensional variables in HG resistance equations can inflate the correlation between the primary variables of interest, and show that the relations found when plotting field data are not spurious.

2.1. Relative-Submergence Resistance Equations

Flow resistance equations for rivers with coarse beds generally contain the dimensionless Chézy-Darcy-Weisbach friction factor f which has the character of a reach-average drag coefficient. It is defined as $f = 8gRS/V^2 \approx 8gdS/v^2$ where g, R, d, S and v are respectively the gravity acceleration, hydraulic radius, mean depth, energy slope, and mean velocity. By rearrangement, $(8/f)^{1/2}$ is also the ratio of mean velocity v to the shear velocity $u_* = (gRS)^{1/2}$. In wide channels $R \approx d$ and in uniform flow the energy slope is the same as the mean water surface slope and mean bed slope. If channel width (w) and slope are known, an estimate of f allows direct prediction of velocity and discharge from depth, or iterative prediction of depth from discharge. The variables v, d and w are the same everywhere in a prismatic channel, but in natural rivers they are often calculated as averages over multiple cross sections (e.g., Bathurst, 1985; Hicks & Mason, 1991).

Most widely-used resistance equations predict $(8/f)^{1/2}$ as a function of the RS d/k or R/k, where k is a roughness height. Generally k is equated with the median grain diameter in the river bed (D_{50}) or a coarse-tail percentile such as D_{84} or D_{90}, but some authors have used the standard deviation (s_z) of vertical departures from the general level of the bed (e.g., Aberle & Smart, 2003). The use of a grain-scale roughness height means that equations of this type are likely to underestimate flow resistance in sand-bed rivers with dunes, or coarse-bed rivers with large woody debris.

Examples that are normally presented in relative-submergence (RS) form include various logarithmic resistance laws with one fitted coefficient (e.g., Bathurst, 1985; Hey, 1979; Keulegan, 1938). Less obviously, the Manning equation can be written as

$$\frac{v}{u_*} = \left(\frac{8}{f}\right)^{1/2} = a\left(\frac{R}{k}\right)^{1/6} \approx a\left(\frac{d}{k}\right)^{1/6} \tag{1}$$

if the Manning coefficient n is assumed proportional to $k^{1/6}$ as proposed by Strickler (1923). A version of this using $d/2D_{90}$ that was introduced by Parker (1991) is widely used by North American researchers, and a version using R/D_{84} forms the deep-flow end member of the VPE proposed by Ferguson (2007):

$$\frac{v}{u_*} = \frac{a_1 a_2 (R/D_{84})}{\left[a_1^2 + a_2^2 (R/D_{84})^{5/3}\right]^{1/2}} \tag{2}$$

The VPE was derived by assuming that the friction factor f is the sum of two components, one obtained by manipulation of Equation 1 and the other by manipulation of a shallow-flow end member

$$\frac{v}{u_*} = \left(\frac{8}{f}\right)^{1/2} = a_2 \frac{R}{D_{84}} \tag{3}$$

The coefficients a_1, a_2 were calibrated using 376 measured values of velocity from various published sources. The best-fit values were slightly different for minimum root-mean-square (rms) error in predictions of v itself (minimum absolute error) or of log v (minimum relative error). Values $a_1 = 6.5$ and $a_2 = 2.5$ were suggested as a compromise giving near-minimum values of both metrics.

2.2. Nondimensional Hydraulic Geometry Equations

A different way to quantify flow resistance is to predict velocity and depth from discharge using a dimensionally consistent HG equation that contains S and k. The term "hydraulic geometry" was introduced by Leopold and Maddock ([1953](#)) as a label for what at the time were empirical, and dimensionally unbalanced, power-law relations describing how the wetted width w, mean depth d, and mean velocity v in a reach vary with the water discharge Q flowing through it. As noted by Ferguson ([1986](#)), at-a-station HG can be understood in terms of geometry and hydraulics: channel cross-section shape determines how d varies with w, flow resistance determines how v varies with d, and because $Q = wdv$ the relations of w, d and v to Q are implicitly determined.

Dimensionally consistent HG equations for flow resistance invert this logic. They use the unit discharge $q = Q/w$ to predict velocity, thereby partitioning q between its components d and v. They can be applied to differences between sites as well as variation over time at one site. In the latter case the need to know how width varies with depth implies that the channel shape is known or assumed. The HG approach does not make explicit use of the friction factor f, and instead includes powers of g, S and k in the prediction equation in order to make the relation between v and q dimensionally consistent. In applications to date the roughness height k has been defined as a grain size (D_{84} or D_{90}), which as already noted may underestimate flow resistance if dunes or large woody debris are present. A potential advantage of the HG approach is that it avoids the need to know the mean flow depth. Depth varies substantially over short distances in many rivers, whereas discharge is constant and width is almost always less variable than depth along a single-thread reach. Scour and fill during floods may make a reach deeper or shallower than at the time of a low-flow survey, but has less or no effect on width. Moreover, it is generally easier to obtain accurate measurements of width than of depth, especially in shallow flows over coarse bed material.

As far as we know the first use of a dimensionally consistent HG equation was by Rickenmann ([1991](#)), who showed that measurements in a very steep flume were fitted quite well by

$$v = 1.3 g^{0.2} S^{0.2} q^{0.6} D_{90}^{-0.4} \tag{4}$$

Aberle and Smart ([2003](#)) found that measurements in a gravel-bed flume followed $(8/f)^{1/2} \propto d/s_z$, which they noted was equivalent to our Equation [3](#) except for the choice of roughness height. The next development was by Comiti et al. ([2007](#)) in an investigation of the bulk hydraulics of a steep step-pool stream. They introduced nondimensional variables

$$v_* = \frac{v}{(gD_{84})^{1/2}} \tag{5a}$$

$$q_* = \frac{q}{(gD_{84}^3)^{1/2}} \tag{5b}$$

and found that their field measurements were fitted fairly well by a power-law relation between v_* and q_*. Zimmerman ([2010](#)), also studying step-pool streams but by means of flume experiments, found that the relative-submergence equations he tried were outperformed by the HG relation $v_* \propto q_*^{0.55} S^{0.32}$.

The mathematical links between HG and RS approaches to flow resistance were clarified by Ferguson ([2007](#)), who showed that the end members of the VPE, Equations [1](#) and [3](#) above, were equivalent to

$$v_* \propto S^{0.3} q_*^{0.4} \tag{6a}$$

for deep flows and

$$v_* \propto S^{0.2} q_*^{0.6} \tag{6b}$$

for shallow flows. Equation 6b is also equivalent to what Rickenmann (1991) and Aberle and Smart (2003) fitted to their flume data. Ferguson (2007) was surprised to find that using Equation 6a for $q_* > 2$ and Equation 6b for $q_* < 2$ gave more accurate predictions of velocity in his data set than the mathematically equivalent Equations 1 and 3 or the VPE that joins them smoothly. He suggested that this paradoxical finding might be because HG equations are more robust to measurement uncertainty in the dependent and predictor variables. We investigate this in Section 6.

Rickenmann and Recking (2011) made a further advance by noting that channel slope could be incorporated into the nondimensional variables introduced by Comiti et al. (2007), to create a new pair of variables:

$$v_{**} = \frac{v}{(gSD_{84})^{1/2}} \tag{7a}$$

$$q_{**} = \frac{q}{(gSD_{84}^3)^{1/2}} \tag{7b}$$

The very large ($n = 2,980$) data compilation assembled by Rickenmann and Recking (2011) was found to follow a gently-curving trend in a log-log plot of v_{**} against q_{**}. Their power-law fit to the trend for $q_{**} > 100$ was almost identical to the 0.4-power relation implied by Equation 6a, but the best fit for $q_{**} < 1$ was steeper (exponent ~0.7) than Equation 6b. Rickenmann and Recking (2011) retained the 0.4-power deep-flow limit case and used logarithmic matching at $q_{**} = 1$ and 100 to obtain two different continuous functions that transition smoothly to alternative shallow-flow limits. Using their own power-law fit for $q_{**} < 1$, they obtained the overall relation

$$v_{**} = \frac{1.5471 q_{**}^{0.7062}}{\left[1 + \left(\frac{q_{**}}{10.31}\right)^{0.6317}\right]^{0.4930}} \tag{8}$$

(their Equation 21). We will refer to this as the RR equation in the rest of the paper. Using instead a 0.6-power shallow limit, they obtained

$$v_{**} = \frac{1.443 q_{**}^{0.6}}{\left[1 + \left(\frac{q_{**}}{43.78}\right)^{0.8214}\right]^{0.2435}} \tag{9}$$

(their Equation 22). The first of these, RR with its steeper lower limit, was used in a comparative test of the ability of different equations to predict measured velocities. The VPE was the best overall of the six relative-submergence equations that were compared, but was outperformed by the new RR relation.

2.3. Statistical Considerations When Evaluating Flow Resistance Equations

In both the RS approach and the HG approach, the x- and y-axis variables in the resistance diagram are compound variables. Velocity is made nondimensional by scaling it by other variables, and its predictor (depth or unit discharge) is likewise made nondimensional by scaling it using one or more other variables. In situations like this, if the same third variable is present in both nondimensional variables, the correlation between the primary variables is inflated. The end-member case is that even in the absence of any causal link or statistical correlation between primary variables x and y, scaling both of them by the same third variable z generates a spurious correlation between x/z and y/z.

A spurious correlation of this type cannot arise in the RS approach, in which v is scaled by $u*$ and d is scaled by k, but in principle it could in the HG approach since v and q are both scaled using S and k. The common dependence on these two variables ensures that the correlation between v_{**} and q_{**} is positive, and inflates its strength. But the correlation is only spurious if the primary variables v and q are uncorrelated. This seems intrinsically unlikely on
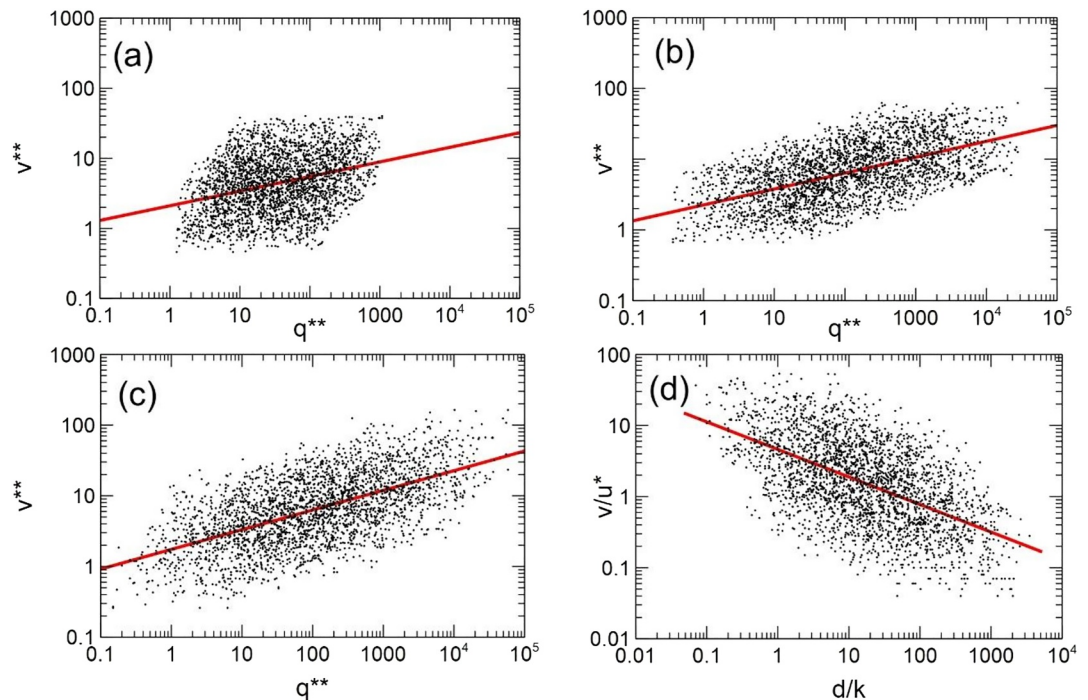
Figure 1. The induced spurious correlation between v^{**} and q^{**} when random numbers are used for q and v. In each plot log q and log v have uniform random distributions with a 100-fold range of q and a 10-fold range of v. In panel (a), slope S is randomly distributed over a 100-fold range but k has a fixed value. In panel (b) S is fixed and k randomly distributed over a 100-fold range. In panel (c) both S and k are randomly distributed over a 100-fold range. Plot (d) shows the implausible relation between v/u^* and d/k in scenario (c). Red lines are best-fit power laws.

physical grounds, but its consequences can be discovered by using random numbers for each of v and q and then adding random variance in S and k.

Figure 1 shows three different randomly-generated $v_{**}-q_{**}$ plots containing the same number of points (2,717) as in the field data set that we analyze later in the paper. In all four plots log q and log v are uniformly distributed and independent, with q in the range 0.1–10 m^2 s^{-1} and v in the range 0.2–2 m s^{-1}. Plots (a), (b) and (c) illustrate three different scenarios about the random variance in S and k. In (a), log S is uniformly distributed with S in the range 0.001–0.1 but k is fixed. In (b), S is fixed but log k is uniformly distributed with k in the range 0.01–1 m. In (c) both S and k vary over these ranges. Plot (d) is the relative-submergence resistance diagram in scenario (c).

This experiment confirms that a totally spurious correlation between v_{**} and q_{**} occurs if v and q are independent of each other and there is variance in S and/or k. Comparison of Figures 1a and 1b shows that k has more effect than S. This is because S is raised to the same power in the definitions of v_{**} and q_{**}, whereas k is raised to different powers and affects q_{**} more than v_{**}. High values of k move a data point rightwards and to a lesser extent upwards, low values move it leftwards and to a lesser extent downwards. This stretches the data out and inflates the correlation coefficient. An important point to note is that the best-fit power law trends shown in Figure 1 all have low exponents (0.20–0.28).

The hypothetical situations in Figure 1 are inconsistent in two ways with the empirical evidence about the physical relations between the primary variables of interest. Firstly, if v and q are uncorrelated, v inevitably has a slight negative correlation with d, and v/u_* (which contains d in the denominator) has a stronger negative correlation with d/k, as illustrated in Figure 1d. These negative correlations are incompatible with boundary-layer physics and with the positive relations found empirically and predicted by RS-type resistance equations. The second inconsistency is that the $v_{**}-q_{**}$ trends in Figure 1 are very different from what is found in HG plots of field data, such as Figure 5a in Rickenmann and Recking (2011) or Figure 3 later in this paper. The ranges of q_{**} and v_{**} in the field data are similar to the randomly-generated ranges in Figure 1c, but the relation of v_{**} to q_{**} in the field

data is nonlinear in log-log space and piecewise best-fit exponents for different parts of the trend are considerably higher than in Figure 1: ~0.6 at low values of q_{**} and ~0.4 at high values.

These discrepancies are conclusive evidence that the v_{**}-q_{**} trends in field data are not totally spurious correlations generated by the definitions of the nondimensional variables in the absence of any underlying correlation between v and q. The correlation between v_{**} and q_{**} is certainly inflated compared to the underlying relation between v and q, but it remains a valid way of visualizing the same physical interconnections between v, d, S and k as in a relative-submergence plot.

In the end, what interests us is the relative skill of the RS and HG approaches at predicting the primary variable(s) of interest: v in the RS approach, v and d in the HG approach. We assess predictive skill using statistical metrics. Taking v as the target variable, and denoting its predicted and measured values as v_p and v_m respectively, three kinds of goodness-of-fit metrics are available: measures of the scatter of v_p–v_m, measures of bias (v_p systematically higher or lower than v_m), and the proportion of predictions that are accurate to within a certain range. Later in the paper we use metrics of all three types: Root-mean-square (rms) prediction error, mean and median prediction error, and the proportion of predictions accurate to within 50%. The rms prediction error in absolute units is influenced mainly by errors in predicting high velocities, associated mainly with deep flows, and is less sensitive to what can be large relative errors (but small absolute errors) in shallow flows. We therefore look also at the rms value of the difference between log v_p and log v_m.

3. Mathematical Links Between RS and HG Flow Resistance Equations

Nondimensional HG equations using v_{**} and q_{**} look quite different from traditional relative-submergence equations, but that does not mean that the two approaches are independent and mutually exclusive. In this section we show that any HG relation between v_{**} and q_{**} that does not involve other variables has an implicit RS equivalent, and conversely that any RS relation that predicts $(8/f)^{1/2}$ from d/k and no other variables has an implicit HG equivalent. If one relation is a simple power law, the other is explicit and also a power law. We use the mathematical links between the two approaches to derive the exact, but implicit, HG equivalent of the VPE. We also derive an explicit HG relation that has the same conceptual basis as the VPE: That the friction factor is the sum of two components.

The mathematical equivalence between RS and HG equations for flow resistance means that both approaches make exactly the same predictions if every variable required to make the prediction is known accurately. But field data on river morphology and bulk hydraulics are seldom completely free of measurement uncertainty, and we show later that the two approaches differ considerably in their sensitivity to measurement error. The same imperfect inputs can then lead to different predictions depending on the type of equation used.

3.1. Mutual Equivalence of HG and RS Resistance Equations

For generality we replace D_{84} in the definitions of v_{**} and q_{**} by k, and assume there is some functional relation between them: $v_{**} = F(q_{**})$. Substituting the identities $q = dv$ and $u* = (gdS)^{1/2}$ then leads to an implicit relation between $v/u*$ and d/k:

$$\frac{v}{u_*} = \left(\frac{k}{d}\right) F\left[\frac{v}{u_*}\left(\frac{d}{k}\right)^{3/2}\right] \tag{10}$$

Thus for any HG relation $v_{**} = F(q_{**})$ that involves no other variables there is an equivalent implicit RS equation that relates v/u_* to d/k.

The reverse of this equivalence can also be proved by noting that the friction factor can be expressed as a function of q_{**} and v_{**} but no other variables: $f/8 = q_{**}/v_{**}^3$. It follows that every different relative-submergence resistance equation that predicts $(8/f)^{1/2}$ from d/k (and no other variable) must have a unique HG equivalent that relates v_{**} to q_{**}. This HG relation will generally be implicit, but in some simple cases it is an explicit equation for v_{**} as a function of q_{**}. In particular, if the relative-submergence relation is the power law

$$\left(\frac{8}{f}\right)^{1/2} = a\left(\frac{d}{k}\right)^b \tag{11a}$$

then there is an equivalent HG power-law relation

$$\frac{v_{**}^{3/2}}{q_{**}^{1/2}} = a\left(\frac{q_{**}}{v_{**}}\right)^b \tag{11b}$$

This simplifies to

$$v_{**} = c q_{**}^m \tag{11c}$$

where $m = (2b + 1)/(2b + 3)$ and $c = a^{2/(3+2b)}$. For example, if the difference between R and d is neglected, the deep- and shallow-flow asymptotes of the VPE (Equations 1 and 3 above) have HG equivalents

$$v_{**} = c_1 q_{**}^{2/5} \tag{12a}$$

for very deep flows, with $c_1 = a_1^{3/5}$, and

$$v_{**} = c_2 q_{**}^{3/5} \tag{12b}$$

for very shallow flows, with $c_2 = a_2^{2/5}$. Equation 12a is the HG equivalent of the Manning equation. Later in the paper we show that it predicts velocity with less error than the traditional relative-submergence version (Equation 1).

3.2. Exact HG Equivalent of the VPE

The approach used to derive eq.11 can be taken to find the exact HG equivalent of a generalized version of the VPE (Equation 2) that uses d/k instead of R/D_{84}. The identities $d/k = q_{**}/v_{**}$ and $f/8 = q_{**}/v_{**}^3$ now lead to

$$v_{**} = \frac{(a_1 a_2)^{2/5} q_{**}^{3/5}}{\left[a_1^2 + a_2^2\left(\frac{q_{**}}{v_{**}}\right)^{5/3}\right]^{1/5}} \tag{13}$$

This exact HG equivalent of the VPE is an implicit equation, requiring an iterative calculation to predict v_{**} from q_{**}. We do this in our tests below, and it may be acceptable for site-specific applications, but it would be inconvenient for use in analytical models. Iterative solutions of Equation 13 with $a_1 = 6.5$ and $a_2 = 2.5$ are within 0.8% of Rickenmann and Recking's Equation 22 (our Equation 9) for all values of q_{**} from 10^{-2} to 10^6, so these relations are essentially interchangeable and Equation 9 is confirmed to be a near-exact and explicit HG equivalent of the VPE throughout the range of RS, and not just at the $q_{**} = 1$ and $q_{**} = 100$ matching points. We will refer to Equation 13 as VPEx hereafter. Later in the paper we show that it predicts velocity with less error than the VPE using d/D_{84}, even though the two equations are mathematically equivalent.

3.3. Conceptually-Equivalent HG Version of the VPE

A new, simple, and explicit HG equivalent of the VPE can be derived by going back to the conceptual basis of the original VPE. As explained above, Ferguson (2007) assumed that the friction factor f is the sum of two components corresponding to the deep and shallow limit cases (Equations 1 and 3 above). Using now the HG equivalents of these asymptotic relations, Equations 12a and 12b, the overall friction factor is found to be

$$\frac{f}{8} = \frac{(c_1^3 + c_2^3 q_{**}^{3/5})}{(c_1^3 c_2^3 q_{**}^{4/5})} \tag{14}$$
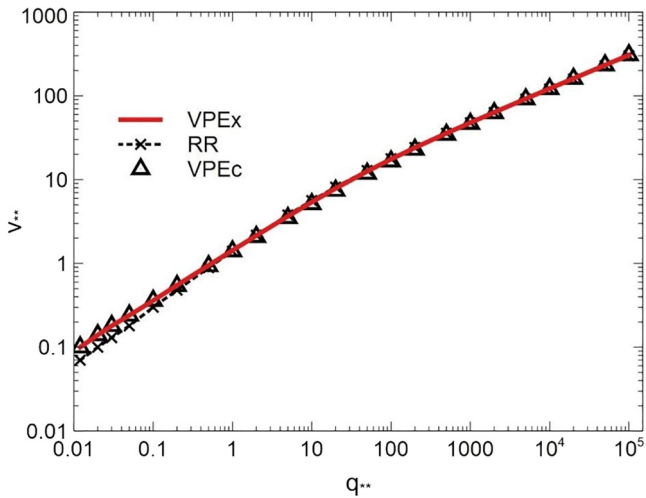
Figure 2. Comparison of the conceptual HG equivalent of the variable-power equation (Equation 15, VPEc) with Equation 13 (VPEx) and Equation 8 (RR).

Using $v_{**} = (8q_{**}/f)^{1/3}$, this leads to a simple explicit relation between v_{**} and q_{**}:

$$v_{**} = \frac{c_1 c_2 q_{**}^{3/5}}{\left(c_1^3 + c_2^3 q_{**}^{3/5}\right)^{1/3}} \tag{15}$$

We will refer to this conceptual equivalent of the VPE as VPEc hereafter. As $q_{**} \to \infty$ the first term in the denominator becomes negligible, which recovers the Manning-style Equation 12a, and as $q_{**} \to 0$ the second term becomes negligible which recovers Equation 12b.

If k is taken as D_{84}, the VPE coefficients $a_1 = 6.5$, $a_2 = 2.5$ proposed by Ferguson (2007) imply $c_1 = 3.07$ and $c_2 = 1.44$. With these values, Equation 15 is indistinguishable from Equation 12 (VPEx) at very small or very high values of q_{**}, and from Equation 8 (RR) at very high values, since they share the same asymptotic relations. At intermediate values Equation 15 predicts slightly lower values of v_{**}, by a maximum of 6% at $q_{**} \sim 50$. When viewed in a log-log graph spanning seven orders of magnitude in q_{**} and more than three in v_{**} (Figure 2), the three relations are indistinguishable except at $q_{**} < 1$ where RR diverges to its different asymptote. At all higher values of q_{**} the maximum difference between RR and the other two relations is 9%.

The VPE coefficients used to compute VPEc in Figure 2 were calibrated using R/D_{84} rather than d/D_{84}, and with a fairly small data set ($n = 376$). Later in the paper we show that the predictive skill of both VPE and VPEc can be improved slightly by recalibrating their coefficients using a much larger data set.

Any prediction of v_{**} from q_{**} is immediately convertible to a prediction of v by using the definition of v_{**}, but in some applications the variable of interest may be the mean depth rather than the mean velocity. It can always be obtained as $d = q/v$, but the VPEc relation can be transformed into a direct prediction equation for d:

$$\frac{d}{k} = \frac{q_{**}^{2/5}\left(c_1^3 + c_2^3 q_{**}^{3/5}\right)^{1/3}}{c_1 c_2} \tag{16}$$

This follows from the identity $d/k = q_{**}/v_{**}$ and has deep-flow and shallow-flow limits $d/k = q_{**}^{3/5}/c_1$ and $d/k = q_{**}^{2/5}/c_2$ respectively. We compare predictions of depth by different resistance equations in Section 5.3.

4. Data Set for Testing and Calibration

A quantitative comparison of the skill of the RS and HG approaches to flow resistance requires measurements of all six relevant variables (S, D_{84}, Q, w, d, v) at a large number of contrasting sites and a range of flow levels. Knowledge of all six variables allows comparison of RS equations that use S, D_{84} and d to predict v (and thus also Q) with HG equations that use S and D_{84} to disaggregate Q/w into its components d and v. Neither approach requires prior knowledge of the target variables. The one target variable that is common to both approaches is v, so we focus on the ability of different RS and HG equations to reproduce the measured velocities at sites in the database.

Our database is an updated version of the one used in Rickenmann and Recking (2011), which was compiled from published sources including an earlier compilation by Church and Rood (1983). The present version includes data from two more sources: Jones and Seitz (1980) and Hicks and Mason (1991). The database was linked to computer code in the R language that was used to select data for analysis, test predictions by different equations, and create graphs illustrating the results. Since we are using a grain size as the roughness height k, we excluded sand-bed rivers ($D_{50} < 2$ mm). In these, flow resistance depends more on the presence/absence and amplitude of dunes than on grain size, and is usually predicted by methods designed to account for large bedforms (e.g., Engelund & Hansen, 1967; Van Rijn, 1984). We also excluded three data sets from channels which the sources describe as containing large woody debris, since allowing for drag on wood is best done in a stress-partitioning approach (e.g., Wilcox et al., 2006).

Table 1
Quality Control Criteria

Maximum difference between Q and wdv	5%
Maximum difference between listed R and $R' = wd/(w+2d)$	−5% and +10%
Minimum w/d	2
Maximum value of Froude number $Fr = v/(gd)^{1/2}$	1.2
Maximum value of v/u_* (% above Keulegan)	30
Minimum value of v/u_* (% below Recking et al., 2008)	30

In many cases the data are incomplete. Sites for which only D_{50} was listed were excluded, and where a source listed D_{90} instead of D_{84} the latter was estimated using D_{50}, D_{90} and the assumption of a lognormal distribution. Some sources report values of the hydraulic radius R as well as mean depth; for those that do not, we estimated it as $R' = wd/(w + 2d)$. Some of the measurements are reach averages based on several surveyed cross sections; others are for single sections in near-uniform reaches. At some sites, particularly on small streams, there are multiple measurements at different discharges, but at others just a single measurement at bankfull discharge.

We performed several quality-control checks on the data using the criteria listed in Table 1 and eliminated measurements that did not pass all checks. The aim was to confirm the mutual consistency and plausibility of the listed values. The identity $Q = wdv$ is central to the HG approach and is also used in most field measurements (v estimated as Q/wd, or Q estimated as wdv), so we discarded measurements in which the identity is not satisfied to within a small tolerance that allows for rounding errors in tabulations. The tolerance in the hydraulic radius test allows for non-rectangular channel shapes but identifies large mismatches between R and d, and the Froude number test identifies major discrepancies between d and v. The two final checks follow Rickenmann and Recking (2011) in excluding values of v/u_* that are either far above a skin-friction prediction using $k = D_{84}$ in a logarithmic law or far below the empirical limit for high flow resistance on steep slopes with intense bedload transport (Equations 29 and 27 of Recking et al., 2008).

After these checks the data set remaining for analysis contained 2,717 separate measurements, 86% of which were also used by Rickenmann and Recking (2011). They span a very wide range of discharge (0.02–15,000 m^3s^{-1}), slope (0.00009–0.18), D_{84} (0.006–2.14 m), depth (0.06–11.2 m), velocity (0.03–5.1 m s^{-1}), and d/D_{84} (0.2–183). Width-to-depth ratios range from 4 to 420 but are predominantly high (mean 36, median 28), so that R and d are interchangeable.

Relative-submergence and HG flow resistance plots of the data are compared in Figure 3. Relatively few reliable measurements exist for large gravel-bed rivers, so the data are mainly from smaller and steeper streams and the median values of Q, S and d/D_{84} are fairly low (4 m^3s^{-1}, 0.015 and 2.1 respectively), but there is a continuous range in both plots.
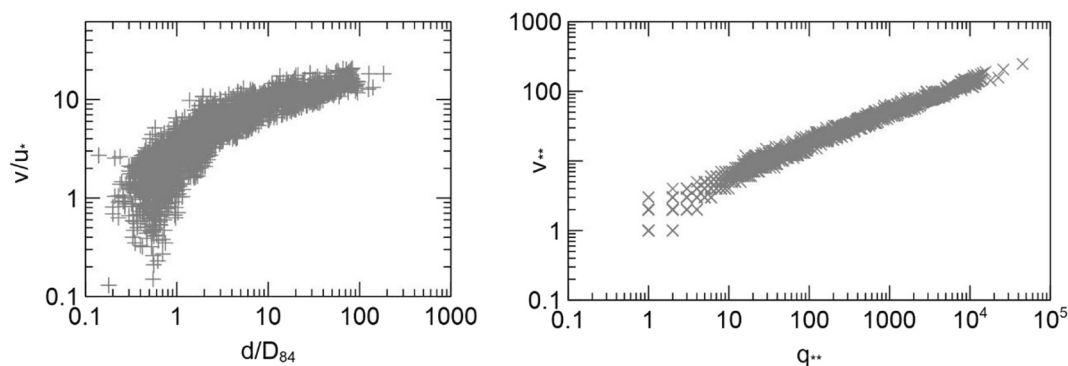

Figure 3. The data set plotted in relative-submergence (left) and nondimensional hydraulic geometry (right) flow resistance diagrams.

Table 2
Flow Resistance Equations Tested in This Paper for Skill in Predicting Measured Mean Velocity

Name used	Source	Eq. no. in this paper	Equation	Coefficient values
MS	Strickler (1923)	1	$v/u_* = a(d/D_{84})^{1/6}$	$a = 8.3$
Keulegan	Keulegan (1938)	–	$v/u_* = 6.25 + 5.75 \log(d/D_{84})$	–
Bathurst	Bathurst (1985)	–	$v/u_* = 4 + 5.62 \log(d/D_{84})$	–
Hey	Hey (1979)	–	$v/u_* = 6.25 + 5.75 \log(d/3.5D_{84})$	–
VPE	Ferguson (2007)	2	$v/u_* = a_1 a_2 (d/D_{84})/[a_1^2 + a_2^2 (d/D_{84})^{5/3}]^{1/2}$	$a_1 = 6.5, a_2 = 2.5$
HGMS	This paper	12a	$v_{**} = c_1 q_{**}^{2/5}$	$c_1 = 3.56$
RR	Rickenmann and Recking (2011)	8	$v_{**} = 1.5471 \, q_{**}^{0.7062}[1 + (q_{**}/10.31)^{0.6317}]^{-0.4930}$	–
VPEx	This paper	13	$v_{**} = (a_1 a_2)^{2/5} q_{**}^{3/5}/[a_1^2 + a_2^2 (q_{**}/v_{**})^{5/3}]^{1/5}$	–
VPEc	This paper	15	$v_{**} = c_1 c_2 q_{**}^{3/5}/[c_1^3 + c_2^3 q_{**}^{3/5}]^{1/3}$	$c_1 = 3.07, c_2 = 1.44$

5. Evaluation of Alternative Resistance Equations

We used the assembled data to (a) test how well different RS and HG equations predict measured velocity, (b) investigate to what extent recalibration improves the performance of some equations, and (c) test how well HG equations predict measured depth.

5.1. Predicting Measured Mean Velocity

The data set was used to evaluate how well velocity is predicted by each of nine flow resistance equations listed in Table 2. Five of them are widely-used RS equations that predict v/u_* from d/D_{84} (though some were initially calibrated using R not d). The other four are HG equations that predict v_{**} from q_{**} with D_{84} used as the roughness scale. Only one equation (RR) was calibrated to a data set that is largely the same as the one used here; the other eight equations are therefore being tested on entirely or predominantly new data. We did not therefore think it necessary to split the data into calibration and validation subsets; we merely note that the RR equation has an advantage over the others.

The predictive skill of each equation is summarized in Table 3, in which v_p/v_m denotes the ratio of predicted to measured velocity. The Hey and Bathurst equations predict negative velocities in very shallow flows; these were replaced by $v_p = 0.01$ m s^{-1} before calculating goodness-of-fit metrics. More detail of the frequency distribution of v_p/v_m for each equation is given in Figure 4.

This analysis confirms three of Rickenmann and Recking's (2011) findings, not surprisingly in view of the big overlap between our data and theirs.

1. The Manning-Strickler and Keulegan equations systematically over-predict velocity in shallow flow conditions and consequently have a strong overall bias and high rms errors. The Hey (1979) log law, Bathurst (1985) log law, and VPE give more accurate predictions with much less overall bias but a wide scatter.
2. The VPE with its default coefficients has the lowest mean and rms errors of the five relative-submergence equations.
3. The two HG equations proposed by Rickenmann and Recking (2011), represented here as RR and VPEx, give considerably smaller prediction errors than any of the relative-submergence equations. In particular, over 99%

Table 3
Accuracy of Velocity Predictions by Alternative Flow Resistance Equations

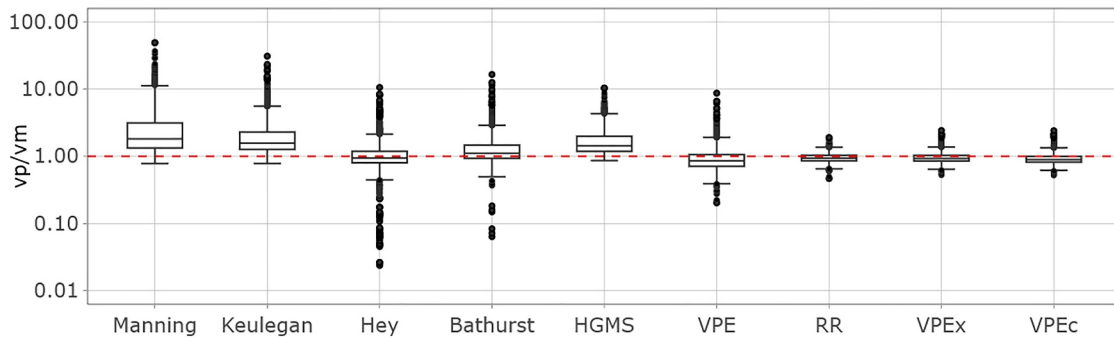|	MS	Keul.	Hey	Bath.	VPE	HGMS	RR	VPEx	VPEc
Mean v_p/v_m	2.82	2.11	1.08	1.36	0.96	1.73	0.96	0.93	0.92
Median v_p/v_m	1.81	1.56	0.94	1.11	0.86	1.43	0.93	0.93	0.89
% v_p/v_m in [0.5, 1.5]	34	45	83	76	88	55	99	99	99
rmse v (m s^{-1})	1.25	0.85	0.37	0.43	0.37	0.55	0.19	0.19	0.22
rmse log v	0.44	0.33	0.22	0.21	0.17	0.26	0.07	0.07	0.08

Figure 4. Box plots of the ratio of predicted to measured velocity for alternative flow resistance equations.

of predictions by VPEx are accurate to ±50%, compared to only 88% for VPE, even though the equations are mathematically equivalent. This difference is illustrated in Figure 5.

Five new findings are that:

4. The performance of the VPE can be improved by recalibration, with rmse reduced to 0.35 m s^{-1} and rmse log to 0.16 by increasing a_1 to 7 and a_2 to 3. This also reduces its already low overall bias, and the new coefficient values improve the already good fit of VPEx,

5. In contrast, the rmse of a Hey-type logarithmic relation is not improved by recalibrating the 3.5 multiplier of D_{84}, and optimisation of the fitted coefficient in the Bathurst equation does not reduce its rms values below those for the VPE.

6. The HG version of Manning-Strickler outperforms the traditional d/D_{84} version, even though they are mathematically equivalent.

7. There is no perceptible difference in predictive skill between RR and VPEx, whereas Rickenmann and Recking (2011) found RR was better. This is probably explained by our omission of channels containing large woody debris, some of which were included in the original analysis and had very low values of both q_{**} and v_{**}.

8. The new VPEc equation (Equation 15) with coefficients converted from those of the VPE has slightly inferior bias and scatter metrics than the earlier HG equations (RR and VPEx). We show later that after calibration it becomes slightly superior in terms of rmse.

Very similar results are obtained if R/D_{84}, not d/D_{84}, is used as the predictor in the relative-submergence equations. The equations that tend to over-predict (Manning, Keulegan) perform slightly better, and the other three perform slightly less well, but the rankings are unchanged. Detailed inspection of the results is possible using the R code used for our computation. As an example, Figure 6 shows how the distribution of v_p/v_m becomes
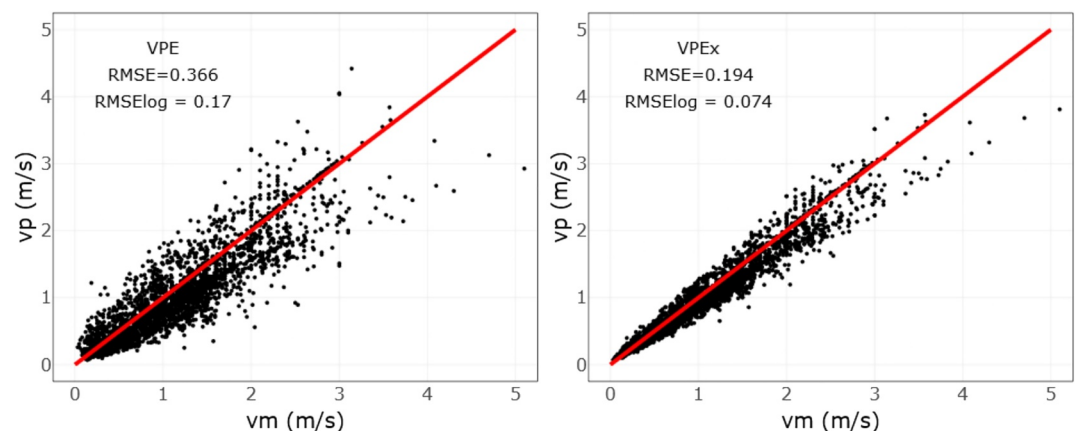

Figure 5. Predicted (v_p) and measured (v_m) mean velocity as obtained using the variable-power equation (left) and its HG equivalent, VPEx (right). Line of equality shown in red.
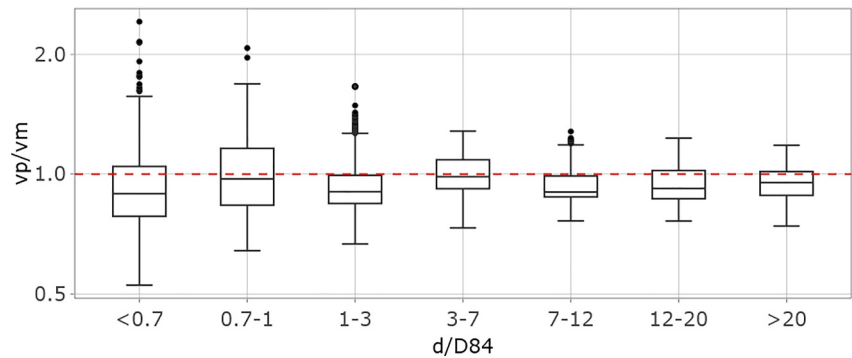
Figure 6. Box plots of prediction errors by VPEx (with its original coefficients) for different ranges of relative submergence d/D_{84}.

wider in very shallow flows. Disaggregation by slope or by q_{**} shows a similar pattern, with wider scatter at steep slopes and at low values of q_{**}. Disaggregation by w/d shows that using depth instead of hydraulic radius in narrow channels is not a problem: predictions using d/D_{84} in VPE, and q_{**} in VPEx, are almost unbiased at $w/d < 10$.

5.2. Calibration of the Conceptual HG Equivalent of the VPE

The results in Table 3 for Equation 15, our new HG flow resistance equation obtained in the same way as the VPE and denoted by VPEc, are for coefficient values $c_1 = 3.07$ and $c_2 = 1.44$. These values were directly converted from the original VPE coefficients $a_1 = 6.5$ and $a_2 = 2.5$, which were calibrated for R/D_{84} not d/D_{84} and using a relatively small data set. We therefore investigated to what extent the d/D_{84} fit to the present much larger data set could be improved.

The rms error in predictions of velocity is reduced from 0.22 to a minimum of 0.17 by increasing c_1 and c_2 slightly, to 3.33 and 1.67 respectively. Alternatively, rmse log is reduced from 0.082 to a minimum of 0.071 with $c_1 = 3.44$ and $c_2 = 1.56$. As a round-number compromise, $c_1 = 3.4$ and $c_2 = 1.6$ gives near-optimal results for both rmse (0.18) and rmse log (0.071), with 98% of predictions accurate to within ±50%. The mean and median values of v_p/v_m become 1.02 and 0.99, showing essentially no overall bias. The VPEc relation with $c_1 = 3.4$ and $c_2 = 1.6$ is therefore marginally better than the existing RR and VPEx equations at reconstructing measured velocity in our database, and far better than any of the relative-submergence equations.

5.3. Prediction of Depth From Discharge

Geomorphological models that involve bedload transport often require a way of estimating the mean bed shear stress for a given water discharge (e.g., Lague, 2010; Parker, 1991; Pitlick et al., 2021). This is almost always done using $\tau = \rho g d S$ with depth estimated by an inverted form of the Manning equation:

$$d = (qn)^{3/5} S^{-3/10} \tag{17a}$$

where n is the Manning friction factor, a value of which has to be assumed. This relation is also used in predictions of local flood risk. If n is equated with $k^{1/6}/(ag^{1/2})$ for dimensional consistency, as in Equation 1, Equation 17a becomes

$$d = (q/a)^{3/5} k^{1/10} (gS)^{-3/10} \tag{17b}$$

This is recognizably a HG relation and is equivalent to

$$d/k = (q_{**}/a)^{3/5} \tag{17c}$$

Table 4
Accuracy of Depth Predictions by Alternative Hydraulic Geometry Flow Resistance Equations

	HGMS	RR	VPEx	VPEc
Mean d_p/d_m	0.67	1.07	1.07	1.00
Median d_p/d_m	0.70	1.07	1.08	1.01
% d_p/d_m in [0.5, 1.5]	75.5	98.9	99.5	99.6
rmse d (m)	0.21	0.21	0.21	0.15
rmse log d	0.26	0.07	0.07	0.07

Note. Predicted and measured depths are denoted by d_p and d_m.

We tested the ability of this equation to reproduce the measured depths in our database. For this purpose we used $k = D_{84}$ and $a = 8.3$, as when testing Manning-Strickler velocity predictions (Tables 2 and 3). For comparison, depth was also predicted using the other three HG relations in Table 2: RR with d predicted as q/v where v is given by Equation 8, VPEx with $d = q/v$ and v from Equation 13, and VPEc with d/k given by Equation 16 and the calibrated coefficients $c_1 = 3.4$ and $c_2 = 1.6$.

Summary results of these tests are shown in Table 4. The HG version of Manning-Strickler has the same rms error in predictions of depth as the less simple RR and VPEx equations, but is severely biased and has a far higher rms log error. This result is what would be expected. For deep flows, with the potential for large prediction errors for depth in meters, the equations are almost the same (HGMS is the asymptote for the other three equations) and are more or less unbiased, but for shallow flows HGMS systematically under-predicts depth and therefore has large relative (but small absolute) errors. The new VPEc equation, with calibrated coefficients, is almost unbiased and has the lowest rms prediction error.

6. Why Are HG Equations Empirically Superior?

We showed above that for any explicit equation predicting v/u_* from d/D_{84} and no other variable, there exists a corresponding relation (possibly implicit) between q_{**} and v_{**}. Conversely, any equation predicting v_{**} from q_{**} and no other variable has a (possibly implicit) d/D_{84} equivalent. In geomorphological models, therefore, where the values of relevant variables are either assumed or modeled, the two approaches are interchangeable and the choice is one of convenience.

The situation is more complicated in applications to real rivers where the relevant predictor variables are measured rather than modeled or assumed. As we noted in Section 3, if all variables are measured accurately, an RS flow-resistance equation makes the same predictions as the HG version of the same equation. However, our tests (Section 5.1) confirm what Ferguson (2007) and Rickenmann and Recking (2011) found: HG predictions of measured mean velocity are substantially more accurate than those using the equivalent RS equation. We think this can only be explained by a combination of two factors: measurement error is present in the test data, and HG equations are less sensitive to it than are RS equations. By implication, HG equations may also be less sensitive to any measurement uncertainty in the variables required to make predictions for rivers not in the test database.

6.1. Sources of Measurement Uncertainty

There are several possible sources of uncertainty in measurements of channel characteristics and bulk flow properties. The required value of S is the energy slope, but in the field it is more usual to measure a reach-averaged center-line bed gradient or water surface slope. These are only identical to the energy slope if the flow is macroscopically uniform and expansion losses are negligible. Even then, some measurement error in slope is possible if the gradient is very low.

D_{84} is obtained from a grain size distribution, which in coarse-bed channels will usually be obtained by pebble count or image analysis. Empirical and theoretical investigations (Eaton et al., 2019; Rice & Church, 1996) suggest that pebble-count estimates of D_{50} and D_{84} have uncertainties of 10%–25% if only 100 pebbles are sampled, which was standard practice at the time of many of our data sources.

If the measured mean depth is based on several surveyed cross sections it should be fairly accurate in large channels with relatively fine bed material. In contrast, a single section will often be unrepresentative of the natural along-reach variability of depth in channels containing pools separated by riffles or steps. Depth measurements in shallow flows over rough beds are imprecise at best and possibly inaccurate, because the point-by-point depth varies greatly over short distances and there is more than one way to define the mean bed level.

Wetted width is generally the variable that can be measured most precisely, but a single section may again be unrepresentative of a reach. Unless the banks are vertical, a width measurement at a single discharge will be incorrect at other discharges leading to error in the estimated unit discharge $q = Q/w$.

The discharge Q is subject to error even at established hydrometric stations. A single current-meter gauging done to ISO standards has an uncertainty of 6% according to Herschy (1999), as reflected in the typical scatter around stage-discharge rating curves. Uncertainty in the fitted rating curve is usually less than this, depending on the number and range of gaugings, but there remains some uncertainty in estimates of Q especially when the rating curve is extrapolated to very low or very high stages.

We take two approaches to investigating whether the HG approach is less sensitive to measurement uncertainty, and if so understanding why. The first approach is analytical, the second empirical.

6.2. Sensitivity to Error: Analytical Considerations

Popular RS flow resistance equations either have a simple power-law form (e.g., Manning-Strickler) or can be represented in variable-power form (e.g., the VPE or a piecewise approximation of a logarithmic relation). If $v/u_* \propto (d/k)^b$, where the exponent b may be constant or variable over the range of RS, we showed earlier that there is an HG equivalent of the form $v_{**} \propto q_{**}{}^m$ and that the exponents are related by $m = (2b + 1)/(2b + 3)$. In the case of the VPE, the deep-flow asymptote is the Manning-Strickler relation with $b = 1/6$ and $m = 2/5$, and the shallow-flow asymptote is $b = 1$ and $m = 3/5$.

Now consider how the predicted value of mean velocity v depends on slope S, roughness height k, and depth d or unit discharge q. In the RS approach,

$$v \propto d^{b+1/2}S^{1/2}k^{-b} \tag{18a}$$

whereas in the HG approach

$$v \propto q^m S^{(1-m)/2}k^{-(3m-1)/2} \tag{18b}$$

For all positive values of b the exponent of S is smaller in Equation 18b than in Equation 18a, implying that an HG prediction of flow resistance is less sensitive to small changes in slope than is a prediction using d/k. In the same way, sensitivity to small changes in the roughness height k is lower in the HG approach for all plausible values of b (to be precise, $0 < b < 0.87$). Likewise, sensitivity to q in Equation 18b is lower than sensitivity to d in Equation 18a.

At $m = 0.5$, which corresponds to an intermediate value of RS, each exponent in Equation 18a is exactly twice its counterpart in Equation 18b. Predictions using data spanning a range from relatively shallow to relatively deep flows are therefore about twice as sensitive to measurement uncertainties when using d/D_{84} as when using q_{**}.

6.3. Sensitivity to Error: Empirical Investigation

To support these theoretical arguments we performed numerical experiments using an "ideal" data set that is fitted perfectly by the VPE in both its d/D_{84} and q_{**} versions. This data set was constructed from the values of Q, w, S and D_{84} in the test data set. From these values we computed v using VPEx and d as q/v. We then investigated how predictions of v from d/D_{84} using the VPE and from q using VPEx are affected by introducing uncertainty to the variables. Three scenarios were considered:

Scenario 1: All variables are obtained independently
Scenario 2: w, d and v are measured and Q is obtained as their product
Scenario 3: Q, w and d are measured and v is obtained as Q/wd.

Scenario 1 is the usual situation for predictions of depth or velocity at a new site, using measurements of (or assumptions about) slope, roughness height, and either depth or unit discharge. Each of these predictor variables is subject to error, but any error in one variable is independent of possible errors in the other two variables.

Scenarios 2 and 3 refer instead to tests of the ability of different resistance equations to reproduce measured velocity. This requires consideration of how "measured" velocity is obtained in practice. Most sites in our database are at or very close to gauging stations, with Q either from the rating curve (nominally scenario 3, but the rating curve is built up from scenario-2 measurements) or from one of the current-meter measurements used to construct the rating curve (scenario 2). Either way, there may be error in any or all of Q, d, v. In contrast to
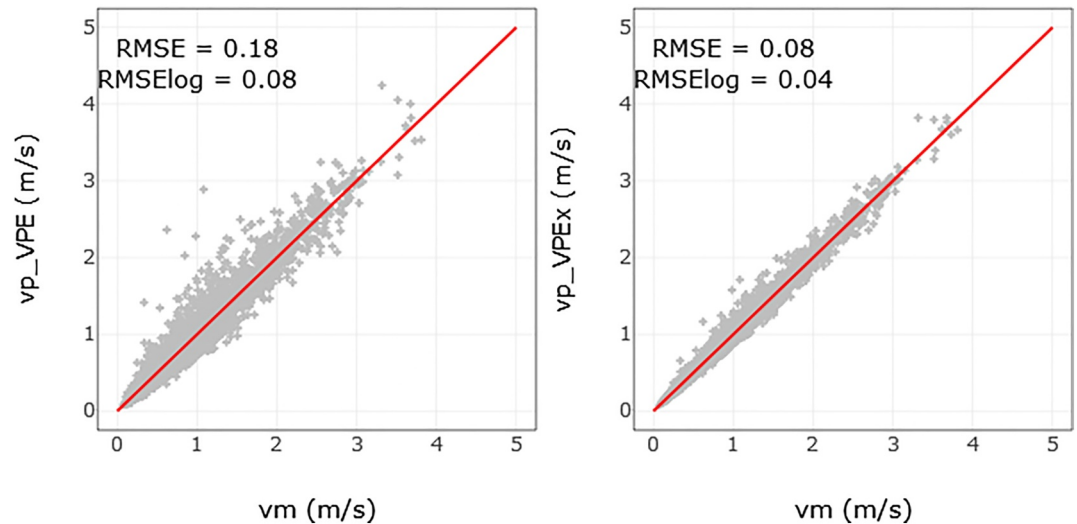
Figure 7. Response of velocity v_m in the "ideal" data set to random perturbation of D_{84} ($\sigma = 25\%$) and S ($\sigma = 10\%$) in scenario 1. Predicted velocity after perturbation is denoted by v_p. Left-hand plot shows calculations from d/D_{84} using variable-power equation, right-hand plot shows calculations from q using VPEx. Line of equality is shown in red.

scenario 1, the errors are now correlated: in scenario 2, any error in d or v causes a proportionate error in Q, and in scenario 3 any error in Q causes a proportionate error in v. At sites away from gauging stations, scenario 2 applies if the bulk flow measurements were obtained by current meter (e.g., Reid & Hickin, 2008). Tracer-wave methods are an alternative to current metering in small streams; estimating v from gulp-wave travel time is scenario 2 and estimating Q from the dilution of a steady or gulp injection is scenario 3.

In each experiment we added random perturbations to one or more variables and examined the extent to which velocity predictions by the d/D_{84} and q_{**} versions of the VPE were affected. The perturbation was a percentage change drawn from a normal distribution with mean zero and a specified percentage standard deviation σ, so that the value x of the variable becomes $x(1 + 0.01z\sigma)$ where z is a random number drawn from the unit normal distribution.

In all scenarios the measurements of S and D_{84} are independent of other measurements, so their effects can be isolated by perturbing just S or just D_{84} without changing q or d. In experiments of this type, velocity predictions by the two methods change in the same direction (upwards with an increase in slope, downwards with an increase in D_{84}) but on average by approximately twice as much when calculated from d/D_{84} as when calculated from q in the HG method. This result is consistent with the analytical considerations in Section 6.2. An example is shown in Figure 7, in which both S and D_{84} are perturbed.

The effects of measurement uncertainty in depth and unit discharge depend on the data-collection scenario. In scenario-1 experiments in which d and q are perturbed to the same extent, both forms of the resistance equation lead to changes in predicted velocity but the predictions using d/D_{84} alter by much more than those using q, consistent with our analytical finding. In scenario 1, therefore, velocity predictions using the HG method are less susceptible to uncertainty in the measurement of each of the four variables S, D_{84}, d and q.

In scenario 2, any error in measuring d or v leads to a proportionate error in $q = dv$. If the velocity measurement is accurate, error in d changes q in the same direction and the HG equation naturally performs better than the d/D_{84} equation, as found in scenario 1. If on the other hand d has been measured accurately but there is error in v, a bias exists because over(under) estimation of v is directly balanced by over(under) estimation of q, which helps an HG equation reproduce the measured (but incorrect) velocity.

These two effects associated with errors in d and v both contribute to the superior performance of HG equations in tests, but it is not possible to unravel their respective weight for lack of precise information on the measurement
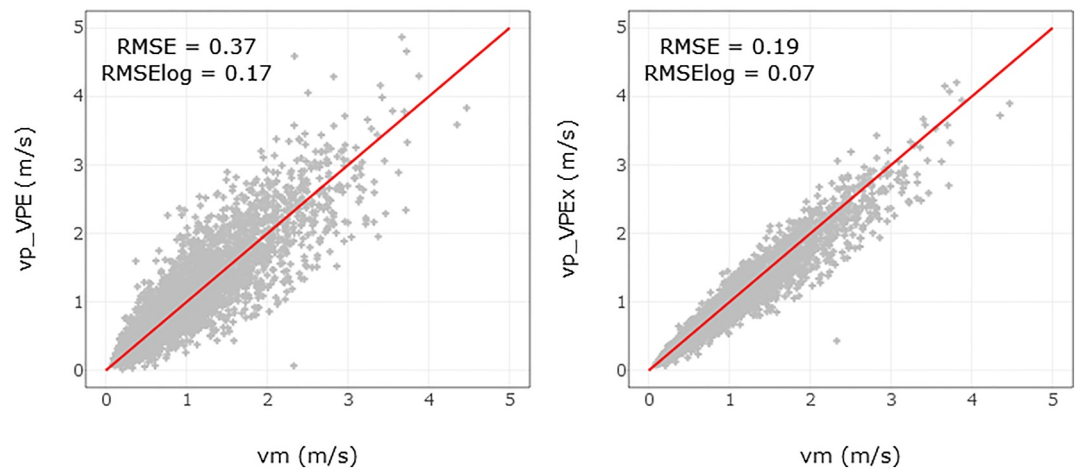
Figure 8. Reconstruction of the real data set evaluation by imposing errors to v, d, S, D_{84} in the ideal data set and assuming scenario 2. Left-hand plot shows predictions using d/D_{84} in the variable-power equation, right-hand plot shows predictions using q in VPEx. Line of equality is shown in red.

uncertainties attached to each variable in our database. However, we can use numerical simulation to estimate the impact of the depth-velocity product on the test scores. The strategy consists in degrading the "ideal" data set in scenario 2 by applying errors to d, v, w, D_{84} and S in order to reconstruct the rmse and rmse log values obtained (Table 2) when testing the VPE and VPEx equations using the real database. A good fit (Figure 8) was obtained with reasonable percentage standard deviations for the perturbations to v (10%), d (23%), S (10%) and D_{84} (25%). No error was applied to w as we are interested in q, the error in which is the product of the error in d and the error in v.

In a second step, the simulation in Figure 8 was repeated with the same σ values but now assuming scenario 1 (independent errors). Because in scenario 2 the error in q is the product of the error in d (23%) and the error in v (10%), we apply in scenario 1 an error in q which is the multiplication of two normal distributions with standard deviations 23% and 10%. The results show that the VPE prediction is unchanged (logically) and the VPEx result is only weakly affected (rmse = 0.21 m s^{-1}, rmse log = 0.08). This suggests the good scores obtained with the HG equations were not (or only weakly) influenced by the potential bias induced by errors in v.

7. Discussion

We have shown that nondimensional HG equations predict mean river velocity more accurately than equivalent equations using the RS d/D_{84}, because the HG version is less sensitive to measurement uncertainty in the variables required for the test. Where HG is appropriate for the problem, therefore, it is to be preferred. We make specific recommendations in our Conclusions (Section 8).

Measurement uncertainty is only one of several sources of scatter in flow resistance plots, and others need to be examined. There are also possible extensions of the HG approach, to other types of river and in connection with advanced measurement technology.

7.1. Sources of Scatter

We have shown that errors in predictor variables add scatter to predictions of velocity by both approaches, but less so when using HG equations. The best-performing equation (VPEc after calibration) reproduces 80% of measured velocities to within ±20% and almost all others to within ±50%. But this is still a substantial scatter, and there are fundamental reasons why the mean velocity of a river cannot be predicted perfectly by a simple equation using only slope, grain size, and mean depth or unit discharge. Even if those variables are free of measurement error, they do not account for several known physical complications. A reach with bar-pool-riffle morphology could have the same mean depth and mean wetted width as a trapezoidal canal, but would not necessarily exert the same

resistance to flow: There are backwater expansion losses in pools, though they diminish at higher discharges. River beds with the same D_{84} can exert different resistance to flow depending on whether the grains are loosely packed or imbricated, and whether there are pebble clusters or boulder steps. During floods, a coarse surface layer may be disturbed and the D_{84} value measured at low flow may no longer be appropriate. High flows are also associated with active bedload transport which increases flow resistance, and scour and fill could alter the flow depth from what is inferred from cross sections surveyed at low flow.

We suspect that only small incremental improvements remain to be made to simple equations for reach-average flow resistance, though additional high-quality data might allow minor recalibration of the best existing equations. Replacing D_{84} by a roughness height based on direct measurement of the topographic roughness of the river bed, as pioneered by Aberle and Smart (2003), has the potential to eliminate one of the complications mentioned above, but as yet few data are available with which to recalibrate resistance equations for the use of s_z or any more elaborate metric. The effect of intense transport on flow resistance was investigated by Recking et al. (2008), who proposed ways of allowing for it, and it may be that improvements can be devised using the ever-increasing quantity of flume and field data on bedload transport.

There are alternative approaches to flow resistance that may be better choices for some applications or particular types of channel. Two-dimensional hydraulic models that predict the spatial distribution of depth-averaged velocity have become standard tools, but they still require assumptions about the global value or spatial distribution of some kind of friction factor. In channels with arrays of large boulders, individual obstacles generate most of the total resistance to flow and a stress-partitioning approach that separates boulder drag from other friction is an option (e.g., Yager et al., 2007). However, drag coefficients for shallowly-submerged or protruding boulders are poorly constrained, and unless the downstream spacing of boulders is high allowance should be made for sheltering effects, possibly using models developed in boundary-layer meteorology (e.g., Macdonald et al., 1998). A stress-partitioning approach may also be preferable in channels with significant quantities of woody debris, or in narrow channels where the banks are significantly rougher or smoother than the bed.

7.2. New Applications

The database used for our tests was deliberately restricted to gravel/boulder bed channels on the grounds that flow resistance in sand-bed rivers often depends more on bedform amplitude than grain size. In an exploratory exercise we computed q_{**} and v_{**} for 264 measurements which we had previously excluded as having $D_{50} \leq 2$ mm. We divided them into two subsets: sand-bed sites with $D_{84} \leq 2$ mm, and sand/gravel sites with $D_{84} > 2$ mm. The sand/gravel sites plotted very close to the curve predicted by VPEc, but the sand-bed sites plotted slightly below it (by a maximum of a factor of 2). This suggests that the sand-bed sites have greater form drag, on average, than is allowed for in the calibration of the HG equation to gravel-bed sites.

There is no reason in principle why HG equations should not also be applicable to bedrock reaches. Most bedrock rivers contain some sediment, and in incised gorges and canyons the sediment typically includes boulders so that RS may be low even when absolute flow depths are high. Using an HG equation with $k = D_{84}$ might then give reasonable predictions. For exposed bedrock, it has become standard practice to use s_z as a roughness height (e.g., Johnson & Whipple, 2007). This metric has the potential to be used in all types of river, and in sand-bed channels it would discriminate between plane beds and bedforms. The coefficients in any equation using s_z would presumably be different from those using D_{84}, and recalibration requires far more data than is currently available on s_z in reaches with flow measurements.

Advances in field measurement technology are opening new possibilities. Most field investigations now routinely include obtaining a digital elevation model from laser scanning or aerial imagery (processed using structure from motion). This opens the way to estimating overall or spatially-distributed roughness and grain size (e.g., Vazquez-Tarrio et al., 2017). Comparable technological advances exist for hydraulics, for example, measurement of surface velocity by particle image velocimetry (Fujita et al., 1998) or radar (Dramais et al., 2013). Image velocimetry and photogrammetry have been successfully used in a flume to validate a map of flow resistance as estimated using the VPE (Piton et al., 2018), and estimation of mean velocity and discharge using only surface measurements (Welber et al., 2016) could be particularly useful during flood events at ungauged sites.

8. Conclusions

We have shown that whatever the definition of roughness height k, any RS equation that predicts v/u_* from d/k and no other variable has an HG equivalent that relates $v_{**} = v/(gSk)^{1/2}$ explicitly or implicitly to $q_{**} = q/(gSk^3)^{1/2}$ and no other variable; the converse is also true.

At first sight this means that an RS equation and its HG equivalent must make identical predictions, but our tests using a large database of flow measurements in coarse-bed streams and rivers do not show this. Instead, dimensionally balanced HG equations predict velocity from unit discharge q much better than relative-submergence equations that predict velocity from d/D_{84}, even when the HG equation is mathematically equivalent to the d/D_{84} equation. Overall, we find that the root-mean-square error in predicting a large set of velocity measurements is reduced by about half when the predictor is q rather than d/D_{84}.

To resolve this paradox, we showed analytically and in numerical experiments that the HG approach is less sensitive to measurement uncertainties in slope and roughness height. It is also less sensitive to uncertainty in d in practical applications where Q is known but v is not. In test cases in which Q is deduced from measured v (so that q contains what is being predicted), the HG fit is only slightly better than when Q is known independently, and that rather spurious improvement is nothing like big enough to explain the hugely better overall fit using HG rather than RS.

We used the mathematical links between RS-type and HG-type equations to derive a new, simple, explicit HG equation using $k = D_{84}$ that has the same conceptual basis as the VPE proposed in Ferguson (2007) and performs better than any existing flow resistance equation in our tests. The generic form of this VPEc relation is Equation 15 in Section 3.2. With $k = D_{84}$ and best-fit coefficients $c_1 = 3.4$, $c_2 = 1.6$ it can be simplified to

$$v_{**} = \frac{1.6 q_{**}^{0.6}}{\left(1 + 0.1 q_{**}^{0.6}\right)^{0.33}} \tag{19}$$

This equation is an effective way to partition a measured, modeled, or assumed value of unit discharge into its components v and d.

For predictions of depth rather than velocity, the VPEc relation in the form of Equation 16 with $k = D_{84}$ and best-fit coefficients simplifies to

$$\frac{d}{D_{84}} = 0.63 q_{**}^{0.4}\left(1 + 0.1 q_{**}^{0.6}\right)^{0.33} \tag{20}$$

At high values of q_{**} (order 10^3 or more), which correspond to d/D_{84} well above 10, this reduces to

$$\frac{d}{D_{84}} = 0.30 q_{**}^{0.6} \tag{21}$$

which is equivalent to the Manning-Strickler relation $v/u_* \propto (d/D_{84})^{1/6}$. Equations 20 and 21 are effective ways to estimate depth or total shear stress from a measured, modeled, or assumed value of unit discharge. They and Equation 19 may be useful in a variety of geomorphological modeling applications, and also for aquatic habitat assessment and river restoration scenarios.

In other applications discharge is not known but depth is known or assumed, as when estimating bankfull discharge or in paleohydrological reconstructions. In this situation a relative-submergence relation is the obvious tool to use. Our tests suggest that the VPE (our Equation 2) is the best available predictor of v and Q from d/D_{84}. Its performance in our test was marginally improved by changing the coefficients a_1, a_2 from 6.5, 2.5 to 7, 3. With the new coefficient values the VPE can be simplified to

$$\frac{v}{u_*} = \left(\frac{8}{f}\right)^{0.5} = \frac{3(d/D_{84})}{\left[1 + 0.18(d/D_{84})^{1.67}\right]^{0.5}} \tag{22}$$

For deep flows this is again equivalent to the Manning-Strickler equation, but unlike that equation it also gives more or less unbiased predictions of velocity in shallow flows.

Our recommendations use D_{84} as the roughness height because that is the most widely-used choice in published sources, which allowed us to assemble the largest possible test data set. The recommended equations are applicable to all flow depths and slopes, and the full range of RS. They are calibrated for rivers with beds of gravel or coarser sediment ($D_{50} > 2$ mm), but we showed in Section 7.2 that they also work well for sand/gravel beds. In principle, they could be recalibrated for alternative definitions of roughness height, possibly based on statistics of the topographic roughness of river beds.

Data Availability Statement

The data and *R* code used in this paper are available on Zenodo: https://zenodo.org/records/14784508.

References

Aberle, J., & Smart, G. M. (2003). The influence of roughness structure on flow resistance on steep slopes. *Journal of Hydraulic Research*, *41*(3), 259–269. https://doi.org/10.1080/00221680309499971

Bathurst, J. C. (1985). Flow resistance estimation in mountain rivers. *Journal of Hydraulic Engineering*, *111*(4), 625–643. https://doi.org/10.1061/(asce)0733-9429(1985)111:4(625)

Church, M., & Rood, K. (1983). *Catalogue of alluvial river channel regime data* (p. 99). Department of Geography, University of British Columbia.

Comiti, F., Mao, L., Wilcox, A., Wohl, E., & Lenzi, M. (2007). Field-derived relationships for flow velocity and resistance in high-gradient streams. *Journal of Hydrology*, *340*(1–2), 48–62. https://doi.org/10.1016/j.jhydrol.2007.03.021

Dramais, G., Le Coz, J., Le Boursicaud, R., Hauet, A., & Lagouy, M. (2013). *Jaugeage par radar mobile: protocole et résultats. SHF Hydrometrie 2013*. SHF.

Eaton, B. C., Moore, R. D., & MacKenzie, L. G. (2019). Percentile-based grain size distribution analysis tools (GSDtools)—Estimating confidence limits and hypothesis tests for comparing two samples. *Earth Surface Dynamics*, *7*(3), 789–806. https://doi.org/10.5194/esurf-7-789-2019

Engelund, F., & Hansen, E. (1967). *A monograph on sediment transport in alluvial streams*. Teknisk Forlag.

Ferguson, R. (2007). Flow resistance equations for gravel- and boulder-bed streams. *Water Resources Research*, *43*(5), W05427. https://doi.org/10.1029/2006WR005422

Ferguson, R. I. (1986). Hydraulics and hydraulic geometry. *Progress in Physical Geography*, *10*, 1–31. https://doi.org/10.1177/030913338601000101

Fujita, I., Muste, M., & Kruger, A. (1998). Large-scale particle image velocimetry for flow analysis in hydraulic engineering applications. *Journal of Hydraulic Research*, *36*(3), 397–414. https://doi.org/10.1080/00221689809498626

Herschy, R. W. (Ed.). (1999). *Hydrometry: Principles and practices* (2nd ed., p. 380). Wiley.

Hey, R. D. (1979). Flow resistance in gravel-bed rivers. *Journal of Hydraulics Division ASCE*, *105*(HY9), 365–379. https://doi.org/10.1061/jyceaj.0005178

Hicks, D. M., & Mason, P. D. (1991). Roughness characteristics of New Zealand rivers. *DSIR Water Resources Survey: Wellington*.

Johnson, J. P., & Whipple, K. X. (2007). Feedbacks between erosion and sediment transport in experimental bedrock channel. *Earth Surface Processes and Landforms*, *32*(7), 1048–1062. https://doi.org/10.1002/esp.1471

Jones, M. l., & Seitz, H. R. (1980). *Sediment transport in the Snake and Clearwater rivers in the vicinity of Lewiston, Idaho*. US Geological Survey, Water Resources Division, (Vol. 80–690). https://doi.org/10.3133/ofr80690

Keulegan, G. H. (1938). Laws of turbulent flow in open channels. *Journal of Research of the National Bureau of Standards*, *21*(6), 707–741. https://doi.org/10.6028/jres.021.039

Lague, D. (2010). Reduction of long-term bedrock incision efficiency by short-term alluvial cover intermittency. *Journal of Geophysical Research*, *115*(F2), F02011. https://doi.org/10.1029/2008JF001210

Leopold, L. B., & Maddock, T. (1953). *Hydraulic geometry of stream channels and some physiographic implications* (Vol. 272, p. 57). US Government Printing Office. https://doi.org/10.3133/pp252

Macdonald, R. W., Griffiths, R. F., & Hall, D. J. (1998). An improved method for the estimation of surface roughness of obstacle arrays. *Atmospheric Environment*, *32*(11), 1857–1864. https://doi.org/10.1016/s1352-2310(97)00403-2

Parker, G. (1991). Selective sorting and abrasion of river gravels. 2. Applications. *Journal Hydraulic Engineering*, *117*(2), 150–171. https://doi.org/10.1061/(asce)0733-9429(1991)117:2(150)

Pitlick, J., Recking, A., Liebault, F., Misset, C., Piton, G., & Vazquez-Tarrio, D. (2021). Sediment production in French Alpine rivers. *Water Resources Research*, *57*(12), e2021WR030470. https://doi.org/10.1029/2021wr030470

Piton, G., Recking, A., Le Coz, J., Bellot, H., Hauet, A., & Jodeau, M. (2018). Reconstructing depth-averaged open-channel flows using image velocimetry and photogrammetry. *Water Resources Research*, *54*(6), 4164–4179. https://doi.org/10.1029/2017WR021314

Recking, A., Frey, P., Paquier, A., Belleudy, P., & Champagne, J. Y. (2008). Feedback between bed load and flow resistance in gravel and cobble bed rivers. *Water Resources Research*, *44*(5), W05412. https://doi.org/10.1029/2007WR006219

Reid, D. E., & Hickin, E. J. (2008). Flow resistance in steep mountain streams. *Earth Surface Processes and Landforms*, *33*(14), 2211–2240. https://doi.org/10.1002/esp.1682

Rice, S., & Church, M. (1996). Sampling surficial fluvial gravels: The precision of size distribution percentile estimates. *Journal of Sedimentary Research*, *66*(3), 654–665. https://doi.org/10.2110/jsr.66.654

Rickenmann, D. (1991). Hyperconcentrated flow and sediment transport at steep slopes. *Journal of Hydraulic Engineering*, *117*(11), 1419–1439. https://doi.org/10.1061/(asce)0733-9429(1991)117:11(1419)

Rickenmann, D., & Recking, A. (2011). Evaluation of flow resistance equations using a large field data base. *Water Resources Research*, *47*(7), W07538. https://doi.org/10.1029/2010WR009793

Strickler, A. (1923). *Beitrage zur Frage der Geschwindigkeitsformel und der Rauhigkeitszahlen für Ströme, kanale, und geschlossene Laitungen.* Mitteilungen Nr.16 des Amtes für Wasserwirtschaft, Eidgenössisches Departement des Innern (p. 77).

Van Rijn, L. C. (1984). Sediment transport, part 1: Bed load transport. *Journal Hydraulic Engineering*, *110*(10), 1431–1456. https://doi.org/10.1061/(asce)0733-9429(1984)110:10(1431)

Vazquez-Tarrio, D., Borgnier, L., Liebault, F., & Recking, A. (2017). Using UAS optical imagery and SfM photogrammetry to characterize the surface grain size of gravel bars in a braided river (Vénéon River, French Alps). *Geomorphology*, 1–13. https://doi.org/10.1016/j.geomorph.2017.01.039

Welber, M., Le Coz, J., Laronne, J., Zolezzi, G., Zamler, D., Dramais, G., et al. (2016). Field assessment of noncontact stream gauging using portable Surface Velocity Radars (SVR). *Water Resources Research*, *52*(2), 1108–1126. https://doi.org/10.1002/2015WR017906

Wilcox, A. C., Nelson, J. M., & Wohl, E. (2006). Flow resistance dynamics in step-pool channels: 2. Partitioning between grain, spill, and woody debris resistance. *Water Resources Research*, *42*(5). https://doi.org/10.1029/2005wr004278

Yager, E. M., Kirchner, J. W., & Dietrich, W. E. (2007). Calculating bed load transport in steep boulder bed channels. *Water Resources Research*, *43*(7), W07418. https://doi.org/10.1029/2006WR005432

Zimmermann, A. (2010). Flow resistance in steep streams: An experimental study. *Water Resources Research*, *46*(9). https://doi.org/10.1029/2009wr007913